Nuclear Instruments and Methods in Physics Research B 366 (2016) 227–233

Contents lists available at ScienceDirect

Nuclear Instruments and Methods in Physics Research B

journal homepage: www.elsevier.com/locate/nimb

Complex cell geometry and sources distribution model for Monte Carlo single cell dosimetry with iodine 125 radioimmunotherapy

F.X. Arnaud [a,b], S. Paillas [c,d], J.P Pouget [c,d,i,j], S. Incerti [e,f], M. Bardiès [g,h], M.C. Bordage [a,b,g,h,*]

[a] Université Toulouse III-Paul Sabatier, INPT, LAPLACE, F-31062 Toulouse, France
[b] CNRS, LAPLACE, F-31062 Toulouse, France
[c] IRCM, Institut de Recherche en Cancérologie de Montpellier, Montpellier F-34298, France
[d] INSERM, U1194, Montpellier F-34298, France
[e] Université Bordeaux, CENBG, UMR 5797, F-33170 Gradignan, France
[f] CNRS, IN2P3, CENBG, UMR 5797, F-33170 Gradignan, France
[g] Inserm, UMR1037 CRCT, F-31000 Toulouse, France
[h] Université Toulouse III-Paul Sabatier, UMR1037 CRCT, F-31000 Toulouse, France
[i] Université de Montpelllier, F-34090 Montpellier, France
[j] Institut régional du Cancer de Montpellier, F-34298 Montpellier, France

ARTICLE INFO

Article history:
Received 26 June 2015
Received in revised form 30 October 2015
Accepted 3 November 2015
Available online 21 November 2015

Keywords:
Monte Carlo
Cellular dosimetry
I-125
Radioimmunotherapy

ABSTRACT

In cellular dosimetry, common assumptions consider concentric spheres for nucleus and cell and uniform radionuclides distribution. These approximations do not reflect reality, specially in the situation of radioimmunotherapy with Auger emitters, where very short-ranged electrons induce hyper localised energy deposition. A realistic cellular dosimetric model was generated to give account of the real geometry and activity distribution, for non-internalizing and internalizing antibodies (mAbs) labelled with Auger emitter I-125. The impact of geometry was studied by comparing the real geometry obtained from confocal microscopy for both cell and nucleus with volume equivalent concentric spheres. Non-uniform and uniform source distributions were considered for each mAbs distribution. Comparisons in terms of mean deposited energy per decay, energy deposition spectra and energy-volume histograms were calculated using Geant4. We conclude that realistic models are needed, especially when energy deposition is highly non-homogeneous due to source distribution.

1. Introduction

Radioimmunotherapy (RIT) is a targeted radionuclide therapy (TRT) modality that combines antibody-binding specificity with the therapeutic effect of short-ranged ionizing radiation on tumour cells. Even though beta particle emitters (with a range of some mm) have been mostly used in that context, alternate radionuclides have been proposed to increase irradiation selectivity and efficacy: alpha particles (range < 100 μm) and Auger electrons (low energy electrons with a range < 1 μm) are currently investigated for small volume disease such as peritoneal carcinomatosis [7]. The advantage of using Auger electrons emitters such as I-125 (intermediate LET 4–25 keV/μm for electrons with energy < 1 keV) in cancer therapy is their short-range (10–500 nm): This insures high cytotoxic effects in tumour cells while sparing non-targeted neighbouring cells (healthy tissues). In addition, sensitive subcellular targets including cell nucleus (for review [29] or cell membrane can be irradiated [23,28,7,21,22].

However, while absorbed dose–effect relationship is well established in conventional external beam radiotherapy (EBRT), the use of short-range particle emitters in TRT requires developing specific radiobiology and dosimetry [16].

Indeed, most of what is known in Radiobiology has been mainly determined with conventional external beam (gamma/X-rays) radiotherapy (CEBRT) or external exposure to alpha particles or ions. The latter Radiobiology cannot be extrapolated because absorbed dose rate in radionuclide therapy depends on the vector, the target and the isotope and is then generally low (<1 $Gy \cdot h^{-1}$). Moreover, exposure is protracted over few hours to days while it is acute in CEBRT, and absorbed dose distribution is highly non-uniform at the cellular but also tissue level while CEBRT delivers homogeneous irradiation in the target area. At last the involvement

* Corresponding author at: Team15, Centre de Recherche en Cancérologie de Toulouse, CRCT, Inserm, UMR1037, Université Toulouse III-Paul Sabatier, Bat A3 Biophysique 133 route de Narbonne, F-31062 Toulouse, France. Tel. +33 616508056.
E-mail address: marie-claude.bordage@inserm.fr (M.C. Bordage).

http://dx.doi.org/10.1016/j.nimb.2015.11.008
0168-583X/

of non-targeted effects, as described for low absorbed doses of external beam irradiation (<0.5 Gy), needs then to be considered [6,25,20] since they may participate significantly to TRT efficacy and may affect the nature of absorbed dose–effect relationships [26,24]. For all these reasons, specific radiobiological effects and dosimetry needs to be investigated in TRT.

The hyper localisation of Auger electrons energy deposition is also an attractive tool to investigate biological effects of ionizing radiations at the subcellular scale but the determination of the absorbed dose (Gy) at the relevant scale is a pre-requisite. Several dosimetric approaches are available to derive absorbed dose at the cellular level – or to cell components:

As long as the mean absorbed dose is a relevant parameter for radiobiology experiments, analytic approaches can be developed to give account of cellular dosimetry [4,5]. The MIRD Committee [13] presented a compendium of S values ($Gy \cdot Bq^{-1} \cdot s^{-1}$) for cellular dosimetry, based on empirical formulas from Cole [10] for electron energy deposition, or an equivalent approach for alpha emitters.

Monte-Carlo modelling of radiation transport has also been proposed and may be more suited at the cellular and especially subcellular scale, as the discrete nature of interactions resulting in energy-loss straggling, angular deflections and secondary electron production may need to be taken into account [12,8].

A very common assumption in cellular dosimetry is to consider concentric spherical cell and nucleus models, associated with uniform sources distribution, which does not reflect the biological reality [9,23]. The impact of geometry on energy deposition at the cellular level has been studied by comparing ellipsoidal geometry versus spherical geometries: the MIRD committee showed that at low energy (down to 5 keV), the impact of geometry on energy deposition cannot be neglected, especially for sources at a distance of the target [13]. More recent studies by Amato et al. confirmed that observation, demonstrating the need for considering realistic geometries [2,3].

Another point to consider is radionuclides distribution non-uniformity. Cellular dosimetry is often performed by assuming uniform radionuclides distribution in the cell, on cell surface, cell cytoplasm or cell nucleus. This approximation is obviously questionable, and to our knowledge, little information is available to challenge that hypothesis. Still, this can have a major impact on dosimetric results especially when considering the very short-range of Auger electrons and the hyper-localisation of energy deposits.

The objective of this work is therefore to evaluate the impact of *cell geometry* and *source distribution* on *energy deposition*, from a realistic biological model used in Auger RIT studies [23,21].

2. Materials and methods

2.1. Cellular model and antibody distribution imaging

2.1.1. Cell line and monoclonal antibodies

Vulvar squamous carcinoma A-431 cells were obtained from ATCC®. A-431 cells expressing the epidermal growth factor receptor (EGFR) were transfected with the gene encoding the carcinoembryogenic antigen (CEA). Then, internalizing m225 (cytoplasmic localisation) and non-internalizing 35A7 (cell membrane localisation) monoclonal antibodies (mAbs) were used as primary antibodies for targeting EGFR and CEA respectively.

The murine m225 mAb (from ATCC) binds to the epidermal growth factor receptor (EGFR/HER1). The non-internalizing murine IgG1k mAb 35A7 is specific for the CEA (Gold 2 epitope, [14,23]. Both m225 and 35A7 mAbs were obtained from mouse hybridoma ascites fluids by ammonium sulphate precipitation followed by ion exchange chromatography on DE52 cellulose (Whatman, Balston, United Kingdom).

The A-431CEA cell line shares common geometric features with most of the colorectal cell lines expressing CEA (HCT 116, LS 174T) that are usually used in 'in vitro' or 'in vivo' experiments.

2.1.2. Cell and source labelling

A-431 cells were plated on 12 mm glass coverslips in culture dishes. Cells were next incubated with anti-CEA or anti-EGFR mAbs for one hour at 37 °C. They were fixed in 3.7% formaldehyde and then permeabilized in 0.1% Triton X-100 for 15 min followed by incubation with 1% PBS/BSA for one hour. To confirm mAb localisation, an Alexa-488-conjugated anti-mouse secondary mAb was used (1:200) (Invitrogen©; Saint Aubin, France). F-actin constituting cytoskeleton was stained with conjugated phalloidin (1:5000) (Sigma–Aldrich) to visualize cell cytoplasm, while nucleus was stained with 0.1 μg/ml Hoechst (Sigma–Aldrich).

After laser excitation, Hoechst emits blue fluorescence at 460–490 nm while Rhodamine–phalloidin emits red light at 630 nm. Anti-CEA and anti-EGFR mAbs antibodies are labelled with an Alexa-530-conjugated anti-mouse secondary mAb which emits at 530 nm in green (Invitrogen©).

2.1.3. Confocal imaging and image processing

Imaging of cell, nucleus and mAbs was then performed using confocal microscopy analysis (Inverse3 Zeiss©) of coverslips using three specific laser wavelengths. Spatial sampling was $0.3 \times 0.3 \times 0.2\ \mu m^3$. An example of A-431 cell geometry and of source distribution is shown in Fig. 1.

Image processing was performed in two automatized steps using imageJ software (http://imagej.nih.gov/ij/).

- The first one allowed cell and nucleus geometry assessment, using signal thresholding in order to remove isolated pixels.
- The second one allowed mAbs distribution assessment, with unspecific signal suppression under a threshold determined from the average pixel value of 20 non-labelled regions of interest inside the cell.

2.2. Impact of cell geometry

2.2.1. Realistic cell model

Following the model presented in the *Geant4 microbeam advanced example* [18], cell and nucleus geometry were made of multiple copies of parallelepiped voxels derived from confocal imaging ($0.3 \times 0.3 \times 0.2\ \mu m^3$). Each individual voxel contains information about its absolute position within the whole cellular

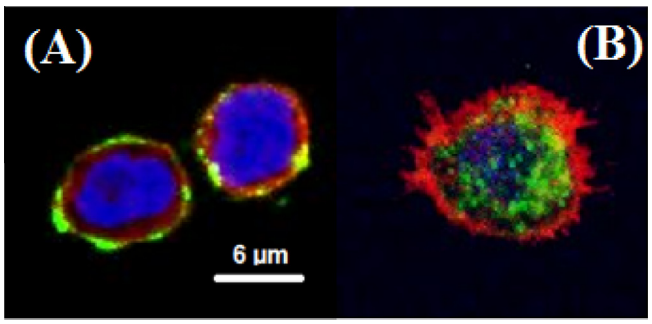

Fig. 1. A-431CEA cell geometry (nucleus in blue, cytoplasm in red) and primary antibody distribution (green) in the medium plane of the cells from confocal imaging (63×). Images were obtained after labelling cytoplasm, nucleus, and 35A7 non-internalizing (left side – A) or m225 internalizing (right side – B) primary antibody. (For interpretation of the references to colour in this figure legend, the reader is referred to the web version of this article.)